



## BALL BEARINGS SUBJECTED TO A VARIABLE ECCENTRIC THRUST LOAD

Mário Ricci

INPE/DMC, São José dos Campos, Brazil, marioesarricci@uol.com.br

**Abstract:** This work introduces a *new*, rapidly convergent, numerical method for internal loading distribution calculation in statically loaded *single-row angular-contact ball bearings* subjected to a known eccentric thrust load, which is applied to a *variable* distance (lever arm or eccentricity) from the geometric bearing centerline. Numerical results for a 218 angular-contact ball bearing have been compared with those from the literature and show significant differences in the magnitudes of the maximum ball load and extend of the loading zone.

**Keywords:** ball, bearing, static, load.

### 1. INTRODUCTION

Ball and roller bearings, generically called rolling bearings, are commonly used machine elements. They are employed to permit rotary motions of, or about, shafts in simple commercial devices such as bicycles, roller skates, and electric motors. They are also used in complex engineering mechanisms such as aircraft gas turbines, rolling mills, dental drills, gyroscopes, and power transmissions.

The standardized forms of ball or roller bearings permit rotary motion between two machine elements and always include a complement of ball or rollers that maintain the shaft and a usually stationary supporting structure, frequently called a housing, in a radially or axially spaced-apart relationship. Usually, a bearing may be obtained as a unit, which includes two steel rings each of which has a hardened raceway on which hardened balls or rollers roll. The balls or rollers, also called rolling elements, are usually held in an angularly spaced relationship by a cage, also called a separator or retainer.

There are many different kinds of rolling bearings. This work is concerned with single-row angular-contact ball bearings (Fig. 1) that are designed to support combined radial and thrust loads or heavy thrust loads depending on the contact angle magnitude. The bearings having large contact angle can support heavier thrust loads. Fig. 1 shows bearings having small and large contact angles. The bearings generally have groove curvature radii in the range of 52-53% of the ball diameter. The contact angle does not usually exceed 40 degrees.

This work is devoted to study of the internal loading distribution in statically loaded ball bearings. Several researchers have studied the subject as, for example, Stribeck [1], Sjövall [2], Jones [3] and Rumbarger [4]. The methods developed by them to calculate distribution of load among the balls and rollers of rolling bearings can be used in most bearing applications because rotational speeds are usually slow to moderate. Under these speed conditions, the

effects of rolling element centrifugal forces and gyroscopic moments are negligible. At high speeds of rotation these body forces become significant, tending to alter contact angles and clearance. Thus, they can affect the static load distribution to a great extension.

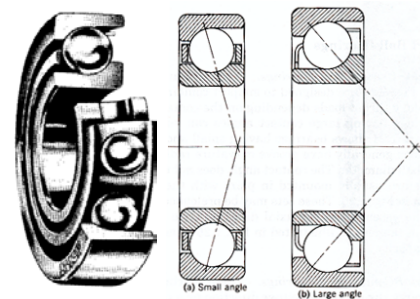


Fig. 1. Angular-contact ball bearing.

The interest here is to describe a method for a specific load distribution consisting of a known eccentric thrust load, which is applied to a *variable* distance (lever arm or eccentricity) from the geometric bearing centerline. Harris [5] described a simplified method for eccentric thrust load calculation based in thrust and moment integrals whose values are obtained from tables or graphics given by Rumbarger, as a function of eccentricity and pitch diameter. The method presented here is more precise theoretically than the method described by Harris, and must be solved iteratively using a digital computer. The difference in accuracy mainly comes from the fact that the first use the pitch radius as lever arm, instead of the inner contact diameter, to have access the Rumbarger's tables and graphics. This obviously introduces an error. At first glance appears that the first method is more attractive than the second because it supplies results more directly whereas no computer is necessary. However, in despite of the simplicity of the former, comparative analyses between results show significant differences in the magnitudes of the maximum ball load and extend of the loading zone.

### 2. SYMBOLS

- $a$  Semimajor axis of the projected contact, m
- $A$  Distance between raceway groove curvature centers, m
- $b$  Semiminor axis of the projected contact, m
- $B$   $f_o + f_i - 1$ , total curvature
- $d$  Raceway diameter, m
- $d_a$  Bearing outer diameter, m
- $d_b$  Bearing inner diameter, m

- $d_c$  Contact diameter, m
- $d_e$  Bearing pitch diameter, m
- $D$  Ball diameter, m
- $e$  Eccentricity of loading, m
- $E$  Modulus of elasticity, N/m<sup>2</sup>
- $E'$  Effective elastic modulus, N/m<sup>2</sup>
- $E$  Elliptic integral of second kind
- $f$  Raceway groove radius  $\div D$
- $F$  Applied load, N
- $k$   $a/b$
- $K$  Load-deflection factor, N/m<sup>3/2</sup>
- $K$  Elliptic integral of first kind
- $M$   $eF_a$
- $P_d$  Diametral clearance, m
- $P_e$  Free endplay, m
- $Q$  Ball-raceway normal load, N
- $r$  Raceway groove curvature radius; solids curvature radius, m
- $s$  Distance between loci of inner and outer raceway groove curvature centers, m
- $R$  Curvature radius; radius of locus of raceway groove curvature centers, m
- $Z$  Number of rolling elements
- $\beta$  Contact angle, rad, °
- $\beta_f$  Free contact angle, rad, °
- $\gamma$   $D \cos \beta / d_e$
- $\Gamma$  Curvature difference
- $\delta$  Deflection or contact deformation, m
- $\Delta\psi$  Angular spacing between rolling elements, rad, °
- $\varepsilon$  Load distribution factor
- $\theta$  Bearing misalignment angle, rad, °
- $\nu$  Poisson's ratio
- $\varphi$  Auxiliary angle
- $\psi$  Azimuth angle, rad, °

Subscripts:

- $a$  Refers to solid  $a$  or axial direction
- $b$  Refers to solid  $b$
- $x,y$  Refers to coordinate system
- $i$  Refers to inner raceway
- $j$  Refers to rolling element position
- $n$  Refers to direction collinear with normal load; integer number
- $o$  Refers to outer raceway
- $t$  Refers to total axial deformation

## 2. GEOMETRY OF BALL BEARINGS

In this section, the principal geometrical relationships for an unloaded ball bearing are summarized. The radial cross section of a single-row ball bearing shown in Fig. 2 depicts the *diametral clearance* and various diameters. The *pitch diameter*,  $d_e$ , is the mean of the inner- and outer-race diameters,  $d_i$  and  $d_o$ , respectively, and is given by

$$d_e = \frac{1}{2}(d_i + d_o). \quad (1)$$

The diametral clearance,  $P_d$ , can be written as

$$P_d = d_o - d_i - 2D. \quad (2)$$

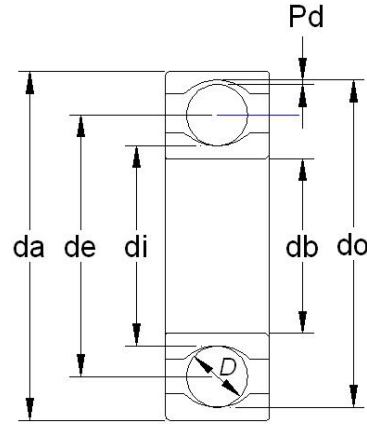


Fig. 2. – Radial cross section of a single-row ball bearing.

*Race conformity* is a measure of the geometrical conformity of the race and the ball in a plane passing through the bearing axis (also named center line or rotation axis), which is a line passing through the center of the bearing perpendicular to its plane and transverse to the race. Fig. 3 depicts a cross section of a ball bearing showing race conformity, expressed as

$$f = r / D. \quad (3)$$

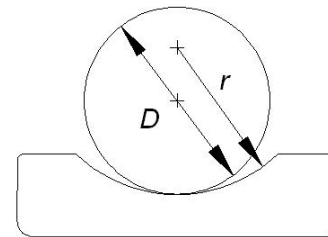
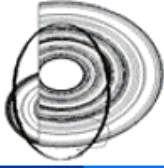


Fig. 3. – Cross section of a ball and an outer race showing race conformity.

Radial bearings have some axial play since they are generally designed to have a diametral clearance, as shown in Fig. 4(a). Fig. 4(b) shows a radial bearing with contact due to the axial shift of the inner and outer rings when no measurable force is applied. The radial distance between the curvature centers of the two races are the same in the Figs. 4(a) and (b). Denoting quantities referred to the inner and outer races by subscripts  $i$  and  $o$ , respectively, this radial distance value can be expressed as  $A - P_d/2$ , where  $A = r_o + r_i - D$  is the curvature centers distance in the shifted position given by Fig. 4(b). Using (3) we can write  $A$  as

$$A = BD, \quad (4)$$



where  $B = f_o + f_i - 1$  is known as the *total conformity ratio* and is a measure of the combined conformity of both the outer and inner races to the ball.

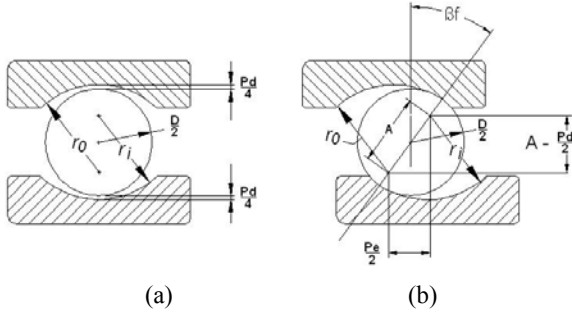


Fig. 4. – Cross section of a radial ball bearing showing ball-race contact due to axial shift of inner and outer rings. (a) Initial position. (b) Shifted position.

The *contact angle*,  $\beta$ , is defined as the angle made by a line, that pass through the curvature centers of both the outer and inner raceways and that lies in a plane passing through the bearing rotation axis, with a plane perpendicular to the bearing axis of rotation. The *free-contact angle*,  $\beta_f$ , (Fig. 4(b)) is the contact angle when the line also passes through the points of contact of the ball and both raceways and no measurable force is applied. From Fig. 4(b), the expression for the free-contact angle can be written as

$$\cos \beta_f = \frac{A - P_d/2}{A}. \quad (5)$$

From (5), the diametral clearance,  $P_d$ , can be written as

$$P_d = 2A(1 - \cos \beta_f). \quad (6)$$

*Free endplay*,  $P_e$ , is the maximum axial movement of the inner race with respect to the outer when both races are coaxially centered and no measurable force is applied. Free endplay depends on total curvature and contact angle, as shown in Fig. 4(b), and can be written as

$$P_e = 2A \sin \beta_f. \quad (7)$$

Considering the geometry of two contacting solids (ellipsoids) in a ball bearing we can arrive at the two quantities of some importance in the analysis of contact stresses and deformations: The curvature sum,  $1/R$ , and curvature difference,  $\Gamma$ , which are defined as

$$\frac{1}{R} = \frac{1}{R_x} + \frac{1}{R_y},$$

$$\Gamma = R \left( \frac{1}{R_x} - \frac{1}{R_y} \right),$$

where

$$\frac{1}{R_x} = \frac{1}{r_{ax}} + \frac{1}{r_{bx}},$$

$$\frac{1}{R_y} = \frac{1}{r_{ay}} + \frac{1}{r_{by}},$$

with  $r_{ax}$ ,  $r_{bx}$ ,  $r_{ay}$  and  $r_{by}$ , being the radii of curvature for the ball-race contact.

A cross section of a ball bearing operating at a contact angle  $\beta$  is shown in Fig. 5. Equivalent radii of curvature for both inner- and outer-race contacts in, and normal to, the direction of rolling can be calculated from this figure. Considering  $x$  the direction of the motion and  $y$  the transverse direction, the radii of curvature for the ball-inner-race contact are

$$r_{ax} = r_{ay} = D/2,$$

$$r_{bx} = \frac{d_e - D \cos \beta}{2 \cos \beta},$$

$$r_{by} = -f_i D = -r_i.$$

The radii of curvature for the ball-outer-race contact are

$$r_{ax} = r_{ay} = D/2,$$

$$r_{bx} = \frac{d_e + D \cos \beta}{2 \cos \beta},$$

$$r_{by} = -f_o D = -r_o.$$

Let

$$\gamma = \frac{D \cos \beta}{d_e}.$$

Then

$$r_{bx} = \frac{D(1 - \gamma)}{2\gamma},$$

$$\frac{1}{R_i} = \frac{1}{r_{ax}} + \frac{1}{r_{bx}} + \frac{1}{r_{ay}} + \frac{1}{r_{by}} = \frac{1}{D} \left( 4 - \frac{1}{f_i} + \frac{2\gamma}{1 - \gamma} \right), \quad (8)$$

$$\Gamma_i = R \left( \frac{1}{r_{ax}} + \frac{1}{r_{bx}} - \frac{1}{r_{ay}} - \frac{1}{r_{by}} \right) = \frac{\frac{1}{f_i} + \frac{2\gamma}{1 - \gamma}}{4 - \frac{1}{f_i} + \frac{2\gamma}{1 - \gamma}}, \quad (9)$$

for the ball-inner-race contact, and

$$r_{bx} = -\frac{D(1 + \gamma)}{2\gamma},$$

$$\frac{1}{R_o} = \frac{1}{r_{ax}} + \frac{1}{r_{bx}} + \frac{1}{r_{ay}} + \frac{1}{r_{by}} = \frac{1}{D} \left( 4 - \frac{1}{f_o} - \frac{2\gamma}{1 + \gamma} \right), \quad (10)$$

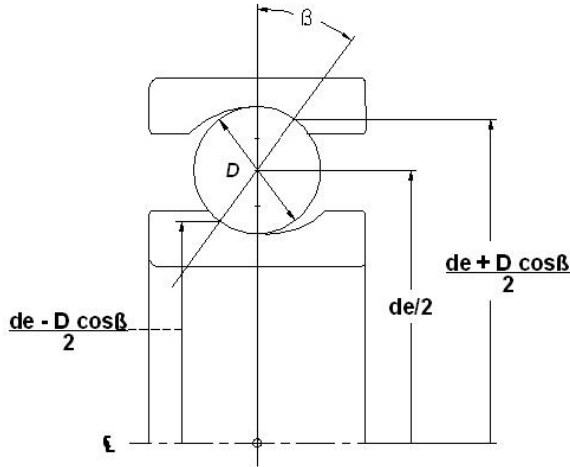


Fig. 5. - Cross section of a ball bearing.

$$\Gamma_o = R \left( \frac{1}{r_{ax}} + \frac{1}{r_{bx}} - \frac{1}{r_{ay}} - \frac{1}{r_{by}} \right) = \frac{\frac{1}{f_o} - \frac{2\gamma}{1+\gamma}}{4 - \frac{1}{f_o} - \frac{2\gamma}{1+\gamma}}, \quad (11)$$

for the ball-outer-race contact.

### 3. CONTACT STRESS AND DEFORMATIONS

When two elastic solids are brought together under a load, a contact area develops, the shape and size of which depend on the applied load, the elastic properties of the materials, and the curvatures of the surfaces. For two ellipsoids in contact the shape of the contact area is elliptical, with  $a$  being the semi-major axis in the  $y$  direction (transverse direction) and  $b$  being the semi-minor axis in the  $x$  direction (direction of motion).

The *elliptical eccentricity parameter*,  $k$ , is defined as

$$k = a/b.$$

From [5],  $k$  can be written in terms of the curvature difference,  $\Gamma$ , and the *elliptical integrals of the first and second kind*,  $\mathbf{K}$  and  $\mathbf{E}$ , as

$$J(k) = \sqrt{\frac{2\mathbf{K} - \mathbf{E}(1 + \Gamma)}{\mathbf{E}(1 - \Gamma)}},$$

where

$$\mathbf{K} = \int_0^{\pi/2} \left[ 1 - \left( 1 - \frac{1}{k^2} \right) \sin^2 \varphi \right]^{-1/2} d\varphi,$$

$$\mathbf{E} = \int_0^{\pi/2} \left[ 1 - \left( 1 - \frac{1}{k^2} \right) \sin^2 \varphi \right]^{1/2} d\varphi.$$

A one-point iteration method, which has been used successfully in the past, is used [6], where

$$k_{n+1} = J(k_n).$$

When the *ellipticity parameter*,  $k$ , the *elliptical integrals of the first and second kinds*,  $\mathbf{K}$  and  $\mathbf{E}$ , respectively, the normal applied load,  $Q$ , Poisson's ratio,  $\nu$ , and the modulus of elasticity,  $E$ , of the contacting solids are known, we can write the semi-major and -minor axes of the contact ellipse and the maximum deformation at the center of the contact, from the analysis of Hertz [7], as

$$a = \left( \frac{6k^2 \mathbf{E} Q R}{\pi E'} \right)^{1/3}, \quad (12)$$

$$b = \left( \frac{6 \mathbf{E} Q R}{\pi k E'} \right)^{1/3}, \quad (13)$$

$$\delta = \mathbf{K} \left[ \frac{9}{2 \mathbf{E} R} \left( \frac{Q}{\pi k E'} \right)^2 \right]^{1/3}, \quad (14)$$

where

$$E' = \frac{2}{\frac{1 - \nu_a^2}{E_a} + \frac{1 - \nu_b^2}{E_b}}.$$

### 4. STATIC LOAD DISTRIBUTION UNDER ECCENTRIC LOAD

Methods to calculate distribution of load among the balls and rollers of rolling bearings statically loaded can be found in various papers [5], [8]. The methods have been limited to, at most, three degrees of freedom in loading and demand the solution of a simultaneous nonlinear system of algebraic equations for higher degrees of freedom. Solution of such equations generally necessitates the use of a digital computer. In certain cases, however – for example, applications with pure radial, pure thrust or radial and thrust loading with nominal clearance – the simplified methods will probably provide sufficiently accurate results.

Having defined a simple analytical expression for the deformation in terms of load in the previous section, it is possible to consider how the bearing load is distributed among the rolling elements. Most rolling-element bearing applications involve steady-state rotation of either the inner or outer race or both; however, the speeds of rotation are usually not so great as to cause ball or roller centrifugal forces or gyroscopic moments of significant magnitudes. In analyzing the loading distribution on the rolling elements, it is usually satisfactory to ignore these effects in most applications. In this section the load deflection relationships for ball bearings are given, along with a specific load distribution consisting of an eccentric thrust load of statically loaded rolling elements.

#### 4.1. Load-Deflection Relationships for Ball Bearings

From (14) it can be seen that for a given ball-raceway contact (point loading)

$$Q = K \delta^{3/2}, \quad (15)$$

where



$$K = \pi k E' \sqrt{\frac{2ER}{9K^3}}$$

The total normal approach between two raceways under load separated by a rolling element is the sum of the approaches between the rolling element and each raceway. Hence

$$\delta_n = \delta_i + \delta_o$$

Therefore,

$$K_n = \left[ \frac{1}{1/K_i^{2/3} + 1/K_o^{2/3}} \right]^{3/2}$$

and

$$Q = K_n \delta_n^{3/2} \quad (16)$$

#### 4.2. Ball Bearings under Eccentric Thrust Load

Let a ball bearing with a number of balls,  $Z$ , symmetrically distributed about a pitch circle according to Fig. 6, to be subjected to an eccentric thrust load. Then, a *relative axial displacement*,  $\delta_a$ , and a *relative angular displacement*,  $\theta$ , between the inner and outer ring raceways may be expected. Let  $\psi = 0$  to be the angular position of the maximum loaded ball.

Fig. 7 shows the initial and final curvature centers positions at angular position  $\psi$ , before and after loading, whereas the centers of curvature of the raceway grooves are fixed with respect to the corresponding raceway. If  $\delta_a$  and  $\theta$  are known, the *total axial displacement*,  $\delta_t$ , at angular position  $\psi$ , is given by

$$\delta_t(\psi) = \delta_a + R_i \theta \cos \psi, \quad (17)$$

where

$$R_i = d_e / 2 + (f_i - 0.5)D \cos \beta_f$$

expresses the locus of the centers of the inner ring raceway groove curvature radii.

Also,

$$\delta_{\max} \equiv \delta_t(0) = \delta_a + R_i \theta. \quad (18)$$

From (17) and (18), one may develop the following relationship

$$\delta_t = \delta_{\max} \left[ 1 - \frac{1}{2\varepsilon} (1 - \cos \psi) \right] \quad (19)$$

in which

$$\varepsilon = \frac{1}{2} \left( 1 + \frac{\delta_a}{R_i \theta} \right). \quad (20)$$

The extend of the *loading zone* is defined by

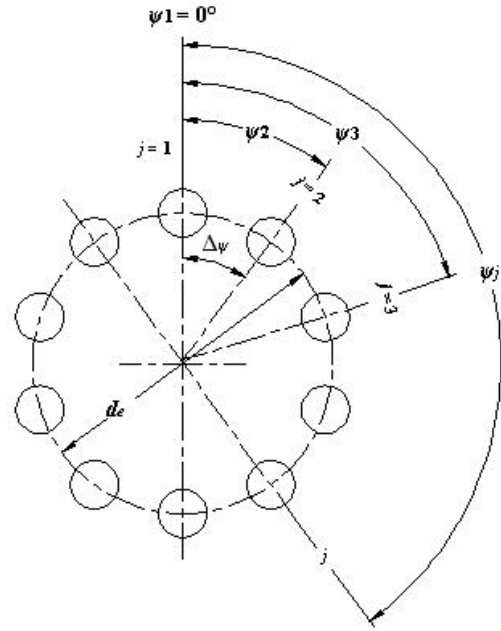


Fig. 6. – Ball angular positions in the radial plane that is perpendicular to the bearing's axis of rotation,  $\Delta\psi = 2\pi/Z$ ,  $\psi_j = 2\pi/Z(j-1)$ .

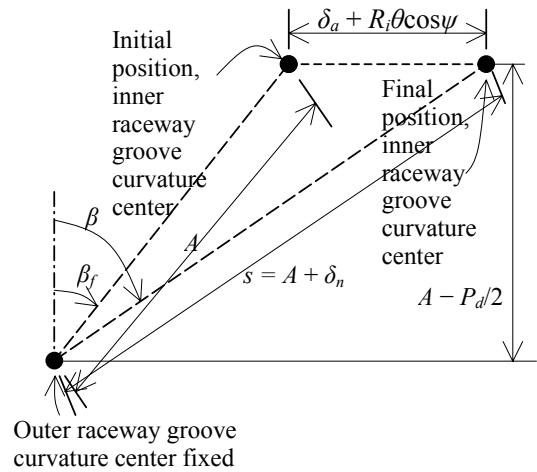


Fig. 7. – Initial and final curvature centers positions at angular position  $\psi$ , with and without applied load.

$$\psi_t = \cos^{-1} \left( \frac{-\delta_a}{R_i \theta} \right). \quad (21)$$

From Fig. 7,

$$\beta(\psi) = \cos^{-1} \left( \frac{A - P_d/2}{A + \delta_n} \right) \quad (22)$$

and

$$\delta_t(\psi) = (A + \delta_n) \sin \beta - A \sin \beta_f. \quad (23)$$

From (5) and (22), the total normal approach between two raceways at angular position  $\psi$ , after the thrust load has been applied, can be written as

$$\delta_n(\psi) = A \left( \frac{\cos \beta_f}{\cos \beta} - 1 \right). \quad (24)$$

From Fig. 7 and (24) it can be determined that  $s$ , the distance between the centers of the curvature of the inner and outer ring raceway grooves at any rolling element position  $\psi$ , is given by

$$s(\psi) = A + \delta_n = A \frac{\cos \beta_f}{\cos \beta}. \quad (25)$$

From (17), (23) and (24) yields, for  $\psi = \psi_j$ ,

$$\delta_a + R_i \theta \cos \psi_j - A \frac{\sin(\beta_j - \beta_f)}{\cos \beta_j} = 0, \quad j = 1, \dots, Z \quad (26)$$

From (16) and (24) yields, for  $\psi = \psi_j$ ,

$$Q_j = K_{nj} A^{3/2} \left( \frac{\cos \beta_f}{\cos \beta_j} - 1 \right)^{3/2}, \quad j = 1, \dots, Z. \quad (27)$$

If the external thrust load,  $F_a$ , is applied at a point distant  $e$  from the bearing's axis of rotation then, for static equilibrium to exist

$$F_a = \sum_{j=1}^Z Q_j \sin \beta_j, \quad (28)$$

$$M = e F_a = \frac{1}{2} \sum_{j=1}^Z d_{cj} Q_j \sin \beta_j \cos \psi_j, \quad (29)$$

where  $d_{cj} \equiv d_e - D \cos \beta_j$ .

Substitution of (27) into (28) yields

$$F_a - A^{3/2} \sum_{j=1}^Z K_{nj} \sin \beta_j \left( \frac{\cos \beta_f}{\cos \beta_j} - 1 \right)^{3/2} = 0. \quad (30)$$

Similarly,

$$e F_a - \frac{A^{3/2}}{2} \sum_{j=1}^Z K_{nj} d_{cj} \cos \psi_j \sin \beta_j \left( \frac{\cos \beta_f}{\cos \beta_j} - 1 \right)^{3/2} = 0. \quad (31)$$

Equations (26), (30) and (31) are  $Z+2$  simultaneous nonlinear equations with unknowns  $\delta_a$ ,  $\theta$  and  $\beta_j$ ,  $j = 1, \dots, Z$ . Since  $K_{nj}$  and  $d_{cj}$  are functions of final contact angle,  $\beta_j$ , the equations must be solved iteratively to yield an exact solution for  $\delta_a$ ,  $\theta$  and  $\beta_j$ .

#### 4. NUMERICAL RESULTS

A numerical method (the Newton-Rhapson method) was chosen to solve the simultaneous nonlinear equations (26), (30) and (31). To show an application of the theory developed in this work a numerical example is presented. I

have chosen the 218 angular-contact ball bearing that was also used by [5]. Thus, the results generated here can be compared to a certain degree with the Harris results.

The Figs. 8 to 10 show some parameters, as functions of the moment,  $M$ , under a 17,800 N applied thrust load.

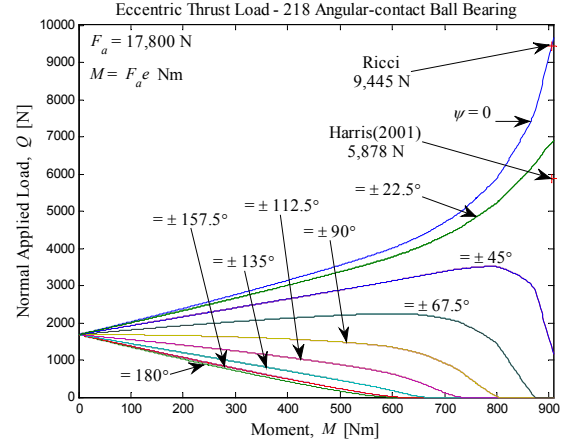


Fig. 8. – Normal ball load,  $Q$ , for 17,800 N thrust load, as a function of the Moment,  $M$ .

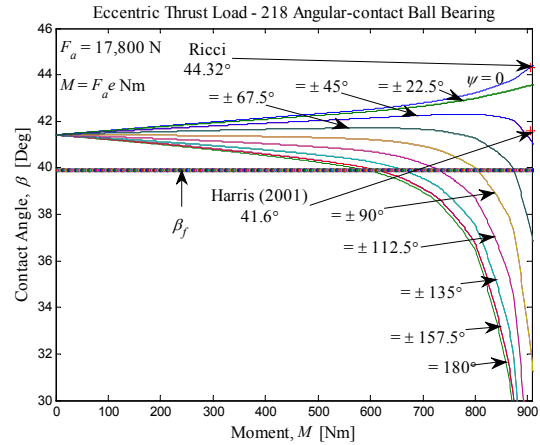


Fig. 9. – Contact Angle,  $\beta$ , for 17,800 N thrust load, as a function of the Moment,  $M$ .

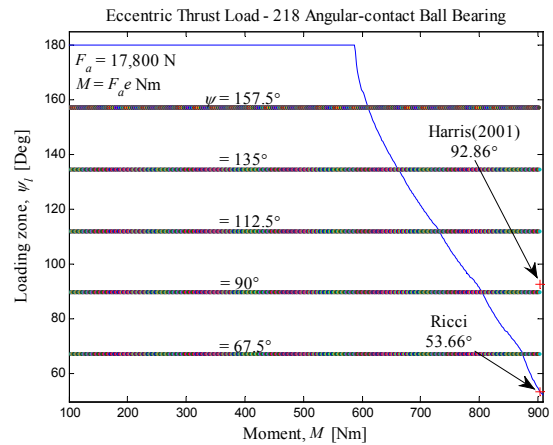
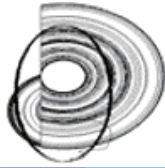


Fig. 10. – Loading zone,  $\psi_i$ , for 17,800 N thrust load, as a function of the Moment,  $M$ .



Figs. 8 to 10 show a substantial difference between results found in this work and those found by Harris for an applied load eccentricity of 50.8 mm. While Harris found a 5,878 N magnitude for the maximum normal ball load (p. 252), this work found a 9,445 N maximum normal ball load. This represents an error of -62.2% in the normal load, meaning that Harris calculation has been underestimated the normal load for the maximum loaded ball.

While Harris has been assumed a contact angle magnitude of  $41.6^\circ$  for all balls (p. 252), contact angles ranging from  $44.317278511598211^\circ$  to  $16.16919216282055^\circ$  were found in this work, while  $\psi$  were varied from  $\psi = 0^\circ$  to  $\pm 180^\circ$ , respectively. This represents errors between -6.1% and +157.3% in the contact angles determination, meaning that Harris calculation has been underestimated (strongly overestimated) the contact angles for balls located at angular positions satisfying  $|\psi| < 45^\circ$  ( $|\psi| > 45^\circ$ ).

While Harris found a loading zone of  $92.86^\circ$  (p. 252), this work found a loading zone of  $53.66^\circ$ . This represents an error of +73% in the loading angle, meaning that the Harris calculation has been underestimated the effect of the moment  $M$ .

## 5. CONCLUSION

A new, rapidly convergent, numerical method for internal loading distribution calculation in statically loaded single-row angular-contact ball bearings subjected to a known eccentric thrust load, which is applied to a *variable* distance (lever arm or eccentricity) from the geometric bearing centerline, has been introduced. The method requires the iterative simultaneous solution of  $Z+2$  simultaneous nonlinear equations with unknowns  $\delta_a$ ,  $\theta$  and  $\beta_j$ ,  $j = 1, \dots, Z$ . Numerical results for a 218 angular-contact ball bearing have been compared with those from the literature and show significant differences in the magnitudes of the maximum ball load and extend of the loading zone.

## ACKNOWLEDGMENTS

I wish to thank Eng. José Pelógia da Silva for have doing the figures 2 up to 6.

## REFERENCES

- [1] Stribeck, R. "Ball Bearings for Various Loads," *Trans. ASME* **29**, 420-463, 1907.
- [2] Sjövall, H. "The Load Distribution within Ball and Roller Bearings under Given External Radial and Axial Load," *Teknisk Tidskrift, Mek.*, h.9, 1933.
- [3] Jones, A. *Analysis of Stresses and Deflections*, New Departure Engineering Data, Bristol, Conn., 1946.
- [4] Rumbarger, J. "Thrust Bearings with Eccentric Loads," *Mach. Des.*, Feb. 15, 1962.
- [5] Harris, T. *Rolling Bearing Analysis*. John Wiley & Sons, Inc., 1966.
- [6] Hamrock, B. J. and Anderson, W. J. "Arched-Outer-Race Ball-Bearing Considering Centrifugal Forces." NASA TN D-6765, 1972.

- [7] Hertz, H. "On the contact of Rigid Elastic Solids and on Hardness," in *Miscellaneous Papers*, MacMillan, London. 163-183, 1986.
- [8] Hamrock, B. J. and Anderson, W. J. *Rolling-Element Bearings*. NASA RP 1105, 1983.